

## Notes

## A-Amylose Single Crystals: Unit Cell Refinement from Synchrotron Radiation Microdiffraction Data

D. Popov,<sup>†</sup> M. Burghammer,<sup>†</sup> A. Buléon,<sup>‡</sup> N. Montesanti,<sup>§</sup> J. L. Putaux,<sup>§</sup> and C. Riekelt\*,<sup>†</sup>

European Synchrotron Radiation Facility, BP 220, F-38043 Grenoble Cedex, France; INRA, Unité Biopolymères, BP 71627 rue de la Géraudière, BP 71627, 44316 Nantes Cedex 3, France; and Centre de Recherches sur les Macromolécules Végétales, ICMG-CNRS, BP 53, F-38041 Grenoble Cedex 9, France

Received January 16, 2006

Revised Manuscript Received March 13, 2006

## Introduction

Up to now, the structure of crystalline polymers has been mostly determined using data that resulted from X-ray fiber diffraction analysis.<sup>1</sup> The random particle orientation results, however, in cylindrically averaged intensities of X-ray fiber diagrams and hence a loss in information depending on the size and symmetry of the specific system. For small unit cells one may choose to refine selected models against the fiber diffraction data. This strategy may, however, bias the result via the introduction of stereochemical information into the refinement process. The growth of polymer single crystals and their study by electron diffraction analysis is one way to achieve a proper deconvolution of X-ray fiber diagrams. In the field of polysaccharides, this technique has led to the revision of several X-ray structures that had been previously determined with the use of X-ray fiber data. Thus, amylose is a linear molecule of (1–4)-linked  $\alpha$ -D-glucopyranosyl units that is found in native starch granules.<sup>2</sup> It can be crystallized in vitro as fibrillar<sup>3</sup> or lamellar crystals<sup>4</sup> that yield X-ray powder diffraction data similar to those of the A and B allomorphs of native starch. Micrometer-sized needle-shaped A-amylose platelet crystals prepared by recrystallization of short amylose chains in dilute solution<sup>4,5</sup> are too small to allow single-crystal X-ray data collection. An X-ray fiber diffraction study of A-amylose was reported by Wu and Sarko in 1978.<sup>3</sup> The subsequent study of micrometer-sized A-amylose single crystals by electron diffraction<sup>5,6</sup> revealed some flaws in the earlier structure determination: (i) a number of reflections were misindexed, and (ii) all the intensities of the diagrams presented a very specific symmetry relationship as only reflections with Miller indices  $h + k + l = 2n$  were present. These observations led to a new refinement of the structure of A-amylose, using the old intensities of Wu and Sarko, but with revised reflection indexation. Packing considerations and selected electron diffraction intensities suggested a monoclinic space group  $B2$  with parallel left-handed double helices, packed in a parallel fashion. These features differed

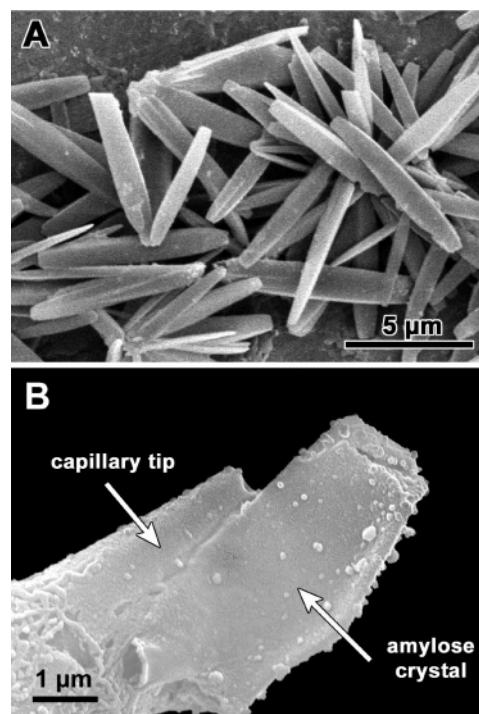


**Figure 1.** (A) SEM image of A-type amylose crystals prepared by recrystallization of synthetic amylose. (B) SEM image of an amylose single crystal (arrow) glued to a borosilicate glass capillary tip. The small ripples on the glass capillary are due to the glue.

from those of the A-amylose structure of Wu and Sarko where an orthorhombic space group and right-handed parallel double helices packed into an antiparallel mode were favored.<sup>3</sup>

Progress in synchrotron radiation (SR) microdiffraction<sup>7</sup> and the preparation of high-quality micrometer-sized A-amylose microcrystals by using short chains of synthetic amylose has now made feasible the collection of X-ray data sets on such very small crystals. The resulting sets are expected to be far superior to the one from electron diffraction where dynamic effects and crystal tilting impart errors to the intensity measurements, which are difficult to correct. In the present Note, we therefore report on SR microdiffraction data collection on single crystals of A-amylose and the use of these data for the refinement of the unit cell and the confirmation of the space group. The structural modifications induced by radiation damage are also presented.

## Experimental Section

**Materials.** Fractions of amylose with a degree of polymerization between 13 and 27 were enzymatically synthesized from sucrose using amylase<sup>8</sup> and subsequently fractionated by high-performance size-exclusion chromatography (HPSEC). Needle-shaped single crystals of A amylose were prepared by recrystallizing dilute aqueous amylose solutions in the presence of acetone vapors, as described elsewhere.<sup>5</sup> A scanning electron micrograph (SEM) of typical crystals is shown in Figure 1A. Air-dried single crystals

<sup>†</sup> European Synchrotron Radiation Facility.

<sup>‡</sup> INRA, Unité Biopolymères.

<sup>§</sup> ICMG-CNRS.

\* Corresponding author.

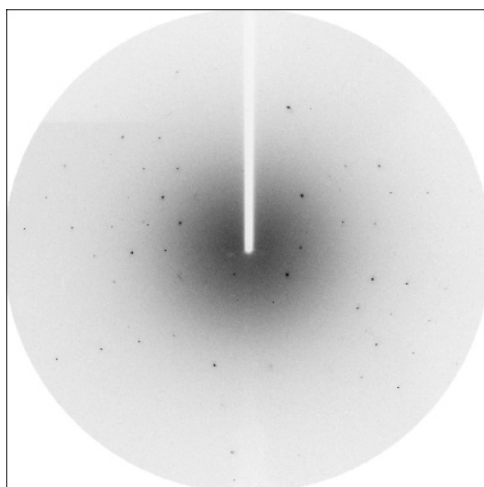


**Figure 2.** Typical X-ray diffraction diagram of single crystal shown in Figure 1B obtained in 5 s for a 5° rotation angle.

**Table 1. Comparison of Intensities of Selected Reflection Pairs, Which Should Be Symmetry-Equivalent According to Orthorhombic ( $I_{hkl} = I_{-hkl}$ ) or Monoclinic ( $I_{hkl} = I_{hk-l}$ ) Symmetries ( $\sigma$  Values in Parentheses)<sup>a</sup>**

symmetry	<i>hkl</i>	<i>I<sub>hkl</sub></i> ( $\sigma$ )	<i>hkl</i>	<i>I<sub>hkl</sub></i> ( $\sigma$ )
orthorhombic	321	2824 (68)	−321	1146 (62)
orthorhombic	411	1709 (55)	−411	3572 (87)
monoclinic	301	5373 (119)	30−1	4929 (109)
monoclinic	121	1012 (62)	12−1	1005 (68)

<sup>a</sup> Orthorhombic unit cell:  $a = 1.7714$  nm,  $b = 1.146$  nm,  $c = 1.055$  nm,  $\alpha = \beta = \gamma = 90^\circ$ ; monoclinic unit cell: Table 2A; column 1.

were attached under an optical microscope by slow setting glue (Araldite) to the tip of a tapered glass capillary using a Kleindiek MM3A micromanipulator (Figure 1B).

**Synchrotron Radiation Experiments.** Experiments were performed at the ESRF ID13 beamline at a wavelength of  $\lambda = 0.0947$  nm defined by a Si-111 monochromator. The beam was focused by parabolic Be refractive lenses<sup>9</sup> and collimated to 10  $\mu$ m at the ID13 microgoniometer.<sup>7</sup> The air-dried crystals were flash-frozen to 100 K using a N<sub>2</sub> cryostream system. Diffraction patterns were recorded by a MAR165 CCD with 2K  $\times$  2K pixels of 78.94  $\times$  78.94  $\mu$ m and 16 bit readout. A typical diffraction pattern is shown in Figure 2. The diffraction patterns were processed using the XDS program package.<sup>10</sup> The micrometer size of the crystals allowed neglecting absorption corrections. Individual scale factors were used to correct for intensity decays in subsequent diffraction patterns. The two crystals studied for the present report were rotated in steps of 2° and 4° with respectively 1 and 2 s exposure time per step. For data analysis reflections with  $I/\sigma(I) \geq 3$  (integrated intensity/

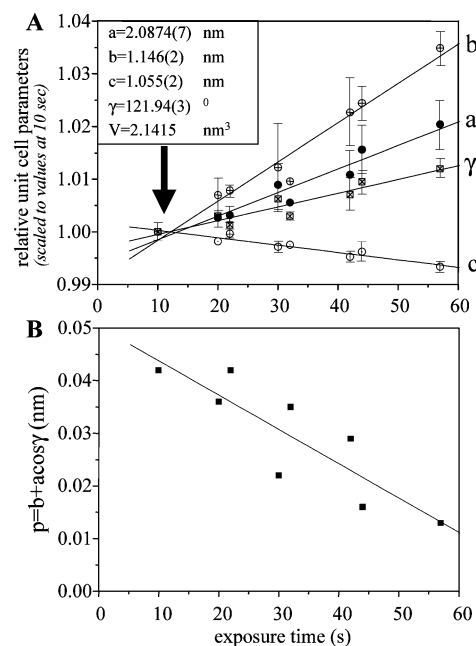


**Figure 3.** (A) Variation of relative unit cell parameters with exposure time for the two crystals investigated ( $2\sigma$  error bars). Data were scaled to unit cell parameters refined at the shortest (10 s) exposure time, which were set arbitrarily to 1.0. (B) Variation of the parameter  $p = b + a \cos \gamma$  with exposure time for the two crystals. The  $p$  value becomes zero for an orthorhombic lattice with monoclinic indexation. The straight lines in (A) and (B) correspond to a linear least-squares fit.

standard deviation) were selected. Radiation damage limited the number of diffraction patterns, which could be analyzed per crystal to 55 and 25 with a total number of statistically significant reflections of 332 and 353, respectively. The highest resolution obtained was 0.151 nm.

## Results and Discussion

The space group was tested using the XDS program package<sup>10</sup> by calculating the merging factor  $R_{\text{int}}$  for the statistically significant reflection intensities:

$$R_{\text{int}} = \left( \sum_h \left[ \sum_i |I_{hi} - \langle I_h \rangle| \right] / \sum_h \langle I_h \rangle \right) \times 100 \quad (1)$$

where  $I_{hi}$  is the  $i$ th observation of the  $h$ th symmetry-equivalent reflection (same intensity imposed by symmetry) and  $\langle I_h \rangle$  the average intensity of the  $h$ th symmetry-equivalent reflection.<sup>11</sup>  $R_{\text{int}}$  and the metrics of the translation lattice favored a monoclinic space group for A-amylose. In the monoclinic setting a value

**Table 2. Comparison of Unit Cell Dimensions and Space Groups from Different Diffraction Experiments ( $\sigma$  Values in Brackets)<sup>a</sup>**

	X-ray single crystal, this work	X-ray powder <sup>5,6</sup>	X-ray fiber <sup>3</sup>	X-ray powder <sup>5,6</sup>	
<i>a</i> (nm)	2.0874 (7)	1.172	1.190	2.125	
<i>b</i> (nm)	1.146 (2)	1.772	1.770	1.172	
<i>c</i> (nm)	1.055 (2)	1.069	1.052	1.069	
$\alpha$ (deg)	90	90	90	90	
$\beta$ (deg)	90	90	90	90	
$\gamma$ (deg)	121.94 (3)	90	90	123.5	
<i>V</i> (nm <sup>3</sup> )	2.1415	2.218	2.216	2.218	
<i>T</i> (K)	100	293	293	100	
possible space groups	monoclinic <i>B2</i>	orthorhombic	orthorhombic	monoclinic <i>B2</i>	
reflections used	57				
<i>N</i>	redundancy	completeness	<i>R</i> <sub>int</sub> (%)	<i>I</i> / $\sigma$ ( <i>I</i> )	<i>R</i> <sub>exp</sub> (%)
55 (1)	1.29 (2)	14.9 (1.8)	3.7 (5.1)	13.46 (3.53)	3.6 (23.6)

<sup>a</sup> The data collection temperature is included. This work: data based on reflections with  $I/\sigma(I) > 3$  up to resolution limit of 0.151 nm. The total data collection time is  $< 10$  s in order to reduce radiation damage effects (Figure 3A,B). The overall reflection statistics derived by XDS<sup>10</sup> is given below. *N*: number of unique reflection; redundancy: total/unique reflections. Values in parentheses correspond to the outer resolution shell (1.51–1.59 Å).

of  $R_{\text{int}} = 7.6\%$  (expected  $R$  value derived from intensity statistics:  $R_{\text{exp}} = 7.0\%$ )<sup>10</sup> was calculated from 263 reflections ( $I/\sigma(I) \geq 3$ ; resolution limit: 0.191 nm), 97 of which are unique. In an orthorhombic setting a value of  $R_{\text{int}} = 19.8\%$  ( $R_{\text{exp}} = 21.9\%$ ) was calculated from 215 reflections ( $I/\sigma(I) \geq 3$ ), 47 of which are unique. This result is based on a large set of symmetry-equivalent reflections and clearly indicates that the symmetry is monoclinic. Table 1 shows for selected pairs of strong symmetry-equivalent reflections that the intensity differences are indeed significantly higher for orthorhombic than for monoclinic setting. The monoclinic space group  $B2$  was chosen as the equally possible space groups  $Bm$  and  $B2/m$  can be excluded on the basis of the optical activity of the A-amylose crystals.<sup>8</sup> In an earlier description,<sup>6</sup> a clear-cut difference between orthorhombic and monoclinic symmetry could not firmly be established. At that time, the monoclinic space group was selected from both biochemical considerations and intensity measurements on  $I_{hkl}$  and  $I_{h-kl}$  pairs from electron diffraction patterns recorded on tilted single crystals. It was not clear whether the observed intensity differences were real or due to slight misalignment of the crystals. The present work is based on X-ray diffraction measurements that are less sensitive to misalignment than those of electron diffraction. The monoclinic space group for A-amylose is therefore firmly established.

A systematic change of unit cell parameters is observed with increasing exposure and hence increasing radiation damage at 100 K (Figure 3A). While the  $a$  and  $b$  parameters and the  $\gamma$  angle were increasing, the  $c$ -axis (chain axis) is decreasing. This observation contradicts therefore the assumption of an exclusively temperature-dependent shrinking of the unit cell.<sup>5</sup> We also note that the monoclinic unit cell got closer to a pseudo-orthorhombic cell ( $\gamma = 123.5^\circ$ )<sup>6</sup> with increasing exposure. This phenomenon can be described using the parameter  $p = b + a \cos \gamma$ , which becomes 0 for a pseudo-orthorhombic lattice (Figure 3B). It would therefore be practically impossible to distinguish a monoclinic from an orthorhombic cell on the basis of powder diffraction data affected by dose-dependent radiation damage. The structure of A-amylose is thought to consist of left-handed, parallel-stranded double helices.<sup>2,6</sup> Radiation damage probably results in hydrogen abstraction and chain scission in the glucopyranosyl units, which will modify the stabilizing hydrogen-bonded network of the double helix and hence the unit cell parameters. A more detailed understanding of this

process will have to await the refinement of the 3D structure of A-amylose, which is in progress.

The unit cell parameters of A-amylose were refined using 57 very well measured strong reflections collected at the shortest exposure time of 10 s. To reduce the influence of radiation damage as far as possible, only reflections collected in a small angular range ( $0-20^\circ$ ) were used. The parameters of the refined monoclinic unit cell are  $a = 2.0874$  nm,  $b = 1.146$  nm,  $c = 1.055$  nm, and  $\gamma = 121.94^\circ$ . A comparison of the unit cell parameters obtained in this study with previously determined values is presented in Table 2. Reflection statistics derived by the XDS program package are also indicated in Table 2.

**Acknowledgment.** The authors thank INSA Toulouse (G. Veronese and M. Remaud) for the gift of synthetic amylose fractions as well as D. Dupeyre (CERMAV) and I. Snigireva (ESRF) for the SEM observations. The authors also thank H. Chanzy for the critical reading of the manuscript and very helpful comments.

## References and Notes

- (1) Tadokoro, H. *Structure of Crystalline Polymers*; Robert E. Krieger Publ. Comp. Inc.: Malabar, 1990.
- (2) Buléon, A.; Colonna, P.; Planchot, V.; Ball, S. *Int. J. Mol. Biol.* **1998**, *23*, 85–112.
- (3) Wu, H. C. H.; Sarko, A. *Carbohydr. Res.* **1978**, *61*, 27–40.
- (4) Buléon, A.; Duprat, F.; Booy, F.; Chanzy, H. *Carbohydr. Polym.* **1984**, *4*, 161–173.
- (5) Imberty, A.; Chanzy, H.; Perez, S.; Buléon, A.; Tran, V. *Macromolecules* **1987**, *20*, 2634–2636.
- (6) Imberty, A.; Chanzy, H.; Pérez, S.; Buléon, A.; Tran, V. *J. Mol. Biol.* **1988**, *201*, 365–378.
- (7) Riekel, C.; Burghammer, M.; Schertler, G. *Curr. Opin. Struct. Biol.* **2005**, *15*, 556–562.
- (8) Potocki-Veronese, G.; Puteaux, J. L.; Dupeyre, D.; Albenne, C.; Remaud-Simeon, M.; Monsan, P.; Buléon, A. *Biomacromolecules* **2005**, *6*, 1000–1011.
- (9) Schroer, C. G.; Kuhlmann, M.; Lengeler, B.; Günzler, T. F.; Kurapova, O.; Benner, B.; Rau, C.; Simionovici, A. S.; Snigirev, A.; Snigireva, I.; Mancini, D. C., Eds.; SPIE: 2002; Vol. 4783, pp 10–18.
- (10) Kabsch, W. In *International Tables for Crystallography*; Rossmann, M. G., Arnold, E., Eds.; Kluwer Academic Publishers: Dordrecht, 2001; Vol. F.
- (11) Rossmann, M. G., Arnold, E., Eds.; *International Tables for Crystallography*; Kluwer Academic Publishers: Dordrecht, 2001; Vol. F, Chapter 9.1.11.4.

MA060114G